PAPER

Check for updates

Microwave-assisted hydrolysis for the physicochemical characterization of functional methacrylic polymers and their bioconjugates

Ilaria Porello, [a] Paola Nastri,[a] Marta Bozzi,[a] Filippo Moncalvo,[a] Philippe Gonzalez,[b] Alessandro Sacchetti [a] and Francesco Cellesi *[a]

This study presents a microwave-assisted hydrolysis (MAH) method for accurately determining the molar mass of functional methacrylic polymers and their protein conjugates synthesized *via* controlled/living polymerization by a grafting from approach. By cleaving ester side chains, MAH converts polymers into linear poly(methacrylic acid) (PMAA), enabling precise molar mass analysis through aqueous size-exclusion chromatography (ASEC). The method is applied to polyglycerol methacrylate (PGMA), polyethylene glycol methacrylate (P(PEGMA)), and lysozyme–PGMA conjugates, with hydrolysis kinetics evaluated under both conventional and microwave heating. Notably, P(PEGMA) exhibits strong resistance to base-catalyzed hydrolysis due to PEG stabilization; however, microwave irradiation significantly improves conversion, achieving results infeasible with standard heating. Characterization by ^{1}H-NMR, FTIR, and SEC confirms successful hydrolysis and accurate molar mass determination. Calibration using PGMA standards further enhances analytical reliability. The MAH–ASEC approach proves robust, scalable, and broadly applicable, offering a valuable tool for the physicochemical characterization of complex polymeric conjugate systems, particularly in biomedical and materials science contexts.

1. Introduction

Microwave-assisted hydrolysis (MAH) is an emerging technique that enhances the efficiency of traditional hydrolysis by using microwave irradiation to accelerate reaction rate.[1–7] This approach enables rapid and uniform heating, significantly reducing both reaction time and energy consumption compared to conventional methods.[8,9] It is particularly effective in breaking down complex biomolecules such as lignocellulosic biomass,[10,11] proteins,[12,13] polysaccharides like starch and chitin[14,15] and synthetic polymers.[16] With increasing interest in green chemistry and sustainable technologies, MAH has found broad application in areas such as biofuel production,[17,18] plastic recycling,[19,20] and pharmaceutical analysis.[21,22] Key advantages of this method include drastically shortened reaction times (from hours to minutes), high energy efficiency, lower reagent usage, and the potential for improved yields and selectivity.[23] MAH can be carried out in three main forms: acid hydrolysis, using strong acids like hydrochloric or sulfuric acid; alkaline hydrolysis, involving bases such as sodium or potassium hydroxide; and enzymatic hydrolysis, which may be

combined with microwave treatment, although enzymes can be sensitive to high temperatures.[24]

Based on these characteristics, MAH can also be employed to optimize or control the hydrolysis of advanced polymeric materials, enabling fast, accurate and reliable physicochemical characterization of the macromolecular chains.[24,25] This is particularly relevant for macromolecules synthesized *via* grafting from approach onto nanoparticles or biosurfaces, cross-linked, or conjugated to large biomolecules such as proteins and nucleic acids in the biomedical field.[26–29] In such cases, detachment from their grafting or conjugation partners is often necessary prior to effective analysis and characterization.[30–33] In the field of polymer–protein conjugate, a method was recently proposed to fully hydrolyse both the side groups of the monomeric units and protein components under strong acidic or basic conditions, allowing isolation of the polymer backbone for molar mass characterization.[3,34,35]

Current analytical strategies for the characterization of engineered polymers such as grafted polymers and polymers with complex self-assembly behavior in solution, often rely on techniques that do not yield accurate or reliable information regarding the real physicochemical properties, in particular the molar mass distribution. The most commonly employed methods for molar mass determination include size exclusion chromatography (SEC), matrix-assisted laser desorption/ionization time-of-flight mass spectrometry (MALDI-TOF MS), analytical ultracentrifugation (AUC), and field-flow

aDepartment of Chemistry, Materials and Chemical Engineering "Giulio Natta", Politecnico di Milano, Via Luigi Mancinelli 7, Milan, 20131, Italy. E-mail: francesco.cellesi@polimi.it

bDepartment of Polymers for Health and Biomaterials, IBMM, Univ Montpellier, CNRS, ENSCM, 34090, Montpellier, France

fractionation (FFF).[36–43] SEC remains the most widely used technique due to its broad applicability, ease of use, and accessibility.[36] However, determining the molecular weight distribution of polymers grafted to a surface is challenging, as their covalently anchored chains cannot be directly analysed by SEC unless they are first detached from the surface. Moreover, SEC can yield inaccurate results when these polymers do not behave as ideal linear coils; the presence of a protein conjugate, self-assembly, folding, or strong intermolecular interactions can distort hydrodynamic volume measurements.[24,44–46]

To address these limitations, one effective approach involves cleave the polymer grafting groups and its side functional groups, thereby isolating the linear polymeric backbone, which can be further analysed through SEC.[24] This approach is possible when the polymer backbone is stable over hydrolysis, for instance in case of polyolephines, polymethacrylates and polyacrylates. In particular, polymethacrylates and polyacrylates have recently been used in a variety of different biomedical applications as a conjugated, grafted, self-assembled macro-molecules, which represent the primary focus of this work.[26,28,29,47,48] At the same time, (meth)acrylic polymers encompass a broad diversity of architectures, functionalities, and processing strategies reported in the literature, including stimuli-responsive materials with tuneable surface properties and multifunctional polymers developed for advanced adhesive and optoelectronic applications.[49,50] In fact, their versatile synthesis via controlled living polymerization techniques such as atom transfer radical polymerization (ATRP),[51,52] reversible addition–fragmentation chain-transfer (RAFT)

polymerization[52–57] or nitroxide-mediated polymerization (NMP),[58,59] have been extensively explored for obtaining polymers exhibiting a narrow molecular weight distribution along with well-defined architectures.[53,60–65]

In particular, these reversible-deactivation radical polymer-izations (RDRP) have allowed extensive research on the use of grafted methacrylic polymers such as poly(ethylene glycol methacrylate) (P(PEGMA)) and poly(glycerol monomethacrylate) (PGMA), for biomedical applications.[26,34,35,52,61,66–70] Their non-toxic nature, hydrophilicity and resistance to protein adsorp-tion make them ideal for drug delivery, tissue engineering, and surface modification of biomaterials, enhancing bi-ofunctionality, stability, and immune compatibility in medical environments.[26,34,35,67–69,71–74] As in many other (meth)acrylic monomers and in the initiators used in these controlled living polymerizations, PGMA and PPEGMA present ester bonds with their functional groups which can be cleaved by hydrolysis.[34,35,66,75–79]

In light of these considerations, this work focuses on developing an effective methodology for characterizing the molar mass of functional polymers synthesized via controlled living polymerization. The approach involves hydrolyzing the ester bonds in their side chains using MAH, thereby yielding linear methacrylate backbones with carboxylic acid on each monomeric unit, namely poly(methacrylic acid) (PMAA), suit-able for subsequent analysis (Fig. 1). Once the molar mass distribution of PMAA is characterized by aqueous SEC, the degree of polymerization, and therefore the molar mass of the polymer prior to hydrolysis, can be easily calculated. The study
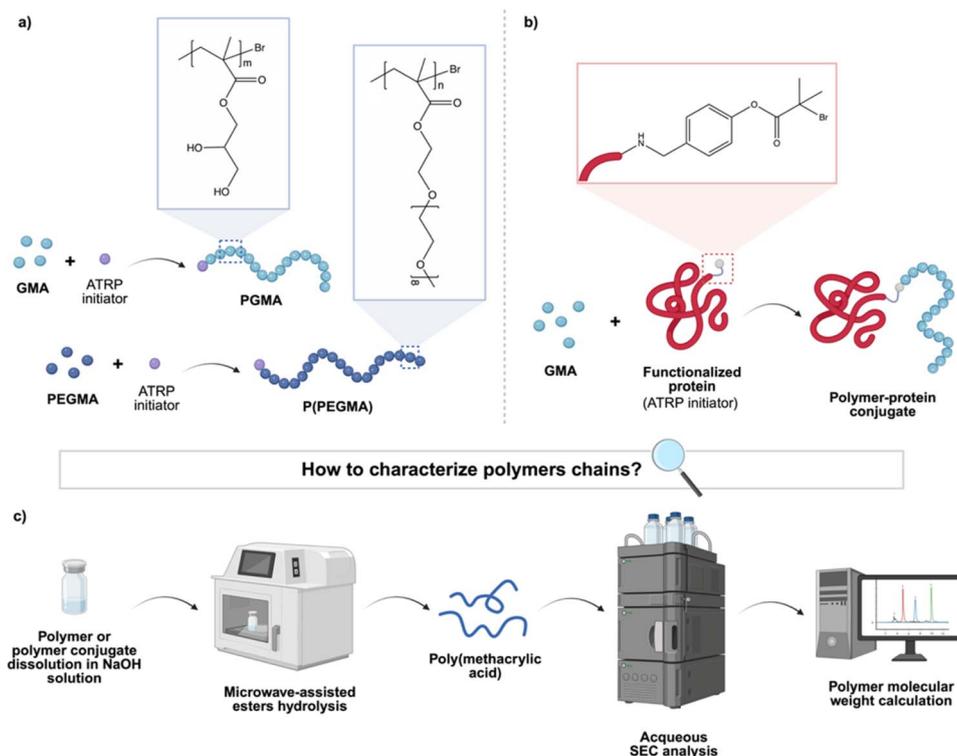

Fig. 1 (a and b) Schematic representation of PGMA or P(PEGMA) and polymer–protein conjugates synthesis via ATRP technique, (c) subsequent polymers hydrolysis via MAH and aqueous SEC characterization.

aimed to optimize the reaction conditions for efficient base-catalyzed hydrolysis, conducted using a microwave synthesizer. To evaluate the hydrolysis kinetics, PGMA was compared with the more sterically hindered P(PEGMA). Two hydrolysis setups were investigated: one using conventional conductive heating (e.g., a silicone oil bath), and the other employing microwave-assisted hydrolysis, the latter expected to accelerate the reaction and improve conversion.

The PGMA and PPEGMA homopolymers investigated in this study were synthesized from a commercial initiator via Activator Generated by Electron Transfer (AGET) ATRP in aqueous solution.[63,80–86] Given the potential of PGMA to form stable polymer–protein bioconjugates, PGMA polymerization was also carried out on functionalized lysozyme, selected as a model protein macroinitiator based on our previous work.[34,35] The bioconjugate was prepared by covalently attaching an aldehyde-bearing ATRP initiator to the N-terminus of lysozyme via reductive amination, targeting a site distal to the active domain to preserve enzymatic activity.[34,35] The resulting PGMA–lysozyme conjugate was then subjected to hydrolysis under the optimized conditions previously established for the corresponding homopolymers,[32,33] enabling characterization of the methacrylate-based polymer. To improve the accuracy of molecular weight determination, a series of PGMA samples with varying chain lengths was employed for calibrating the aqueous SEC analysis, reducing the systematic errors typically associated with standard calibrations using commercial polymer calibrants.[40,87,88]

Here, MAH is introduced as an integral step of an analytical workflow rather than as a synthetic tool. Polymer-derived internal calibrants are first generated from polymers with known molar mass and subsequently applied to the characterization of structurally related functional polymers and bioconjugates with unknown molar mass, overcoming intrinsic limitations of conventional SEC calibration arising from differences in polymer chemistry, charge density, and hydrodynamic volume.

2. Experimental

2.1. Materials

2-Hydroxyethyl 2-bromoisobutyrate 95% (OH-EBIB), Poly (ethylene glycol) methyl ether methacrylate M_n = 500 Da (PEGMA), Lysozyme from hen egg white protein ≥90%, ≥40.000 units per mg protein lyophilized powder (LYS), copper(II) bromide 99% ($CuBr_2$), copper(II) chloride 97.0% ($CuCl_2$), L-ascorbic acid crystalline ≥ 99.0% (AA), 2-methylpyridine borane complex 95%, lithium bromide 99% anhydrous (LiBr), sodium chloride ≥ 99.8% (NaCl), sodium hydroxide ≥ 98.0% anhydrous pellets (NaOH), sodium dihydrogen phosphate ≥ 98.0% anhydrous (NaH_2PO_4), sodium phosphate dibasic ≥ 99.0% (Na_2HPO_4), dimethyl sulfoxide ≥ 99.7% (DMSO), hydrochloric acid 37% (HCl), were all purchased from Sigma-Aldrich (Merck, Italy). Deuterium oxide 100% (D_2O) was purchased from Eurisotop (Cambridge Isotope Laboratories, France). N,N-dimethylacetamide HPLC grade 99.5% (DMAc) was purchased from ThermoFisher Scientific (Italy). Glycerol

mono methacrylate M_n = 176.2 Da (GMA) was purchased from Polysciences (Germany). Tris (2-pyridylmethyl) amine 98% (TPMA) was purchased from Tokyo Chemical Industry (Belgium). All chemicals were used without further purification unless otherwise indicated. Deionized water (18.2 MΩ) was obtained from Millipore Milli-Q purification unit (Merck Millipore).

2.2. Polymers characterization

Monomers conversion (χ_{ATRP}) and hydrolysis outcomes (χ_{HYDRO}), together with polymer degree of polymerization (DP) were determined by ^{1}H-NMR analysis, dissolving crude and purified polymers in D_2O. ^{1}H-NMR spectra were recorded at 298 K on a Bruker Avance 400 MHz instrument (16 scans, standard 1D proton experiment). Chemical shifts (δ) are reported in ppm downfield from the deuterated solvent used as internal standard.

The number-average molar mass ($M_{n,SEC}$) and dispersity ($Đ_{SEC} = M_{w,SEC}/M_{n,SEC}$) values of the synthesized polymers were evaluated using a Jasco® LC-2000Plus size exclusion chromatography (SEC) instrument equipped with a refractive index detector (RI-2031Plus, Jasco), a CO-2060 plus oven column, a PU-2080 pump, a Jasco AS-2055Plus autosampler, 3 × GRAM columns (300 × 8 mm, 10 μm) and 1 × GRAM column guard (50 × 8 mm, 10 μm) using DMAc (30 mM LiBr) as eluent. The machinery was calibrated via polystyrene standards (calibration kits by RESTEK and Sigma-Fluka). Samples of purified polymer were dissolved in DMAc at a concentration of 4 mg mL^{-1}, filtered through Corning® syringe filters (Nylon membrane, pore size 0.45 μm, Merck Millipore) and injected at a flow rate of 1 mL min^{-1} at 35 °C (injection volume = 30 μL).

The hydrolyzed polymers were analyzed via aqueous SEC (ASEC) conducted on a Shimadzu Nexera LC system equipped with a LC-40D pump (Shimadzu), a DGU-403 degassing unit (Shimadzu), a SIL-40 autosampler (Shimadzu), a CTO-40C column oven (Shimadzu), 1 × Agilent PL aquagel-OH guard column (50 × 7.5 mm, 8 μm), 2 × Agilent PL aquagel Mixed-M column (300 × 7.5 mm, 8 μm), a RID-20A refractive index detector. The mobile phase was composed of 0.2 M $NaNO_3$, 0.1 M NaH_2PO_4 (pH 7), and 200 ppm NaN_3. The flow rate was set at 1 mL min^{-1} (injection volume = 100 μL at a concentration of 5 mg mL^{-1}). The number-average and weight-average molar masses ($M_{n,ASEC}$ and $M_{w,ASEC}$, respectively) and the dispersity ($Đ_{ASEC}$) were expressed according to calibration using poly(ethylene glycol) (PEG) standards.

Samples of both native and hydrolyzed polymers where additionally analyzed via Fourier Transform Infrared (FTIR) spectroscopy using a Varian 640-IR spectroscope with ATR-50i accessories and a diamond window. FTIR spectra were collected in ATR mode over the range 4000–600 cm^{-1}, with a resolution of 4 cm^{-1} and averaging 32 scans per spectrum.

2.3. Synthesis of PGMA$_m$ from commercial initiator

100 mL of PBS 100 mM were inserted in a two-necks round bottom flask, 3 cycles of vacuum/N_2 of 5 min each were performed followed by 15 min of N_2 purge. All reactants were used

in the molar ratios reported below, expressed as equivalents with respect to the ATRP initiator. GMA monomer (200 mg, 1.25 mmol, m eq., where $m = 20, 50, 80, 125$) was inserted in a Schlenk vial and 3 vacuum/N_2 cycles of 5 min each were performed. 7.6 mL of degassed PBS 100 mM were added to the Schlenk vial, and the reaction mixture was left under continuous flow of N_2. Considering as general case the polymerization where $m = 125$, the catalyst $CuCl_2$ (0.1012 mg, 0.00075 mmol, 0.075 eq.) and the ligand TPMA (1.7477 mg, 0.006 mmol, 0.6 eq.) were added to the reaction mixture from a stock solution in PBS 100 mM ([$CuCl_2$] = 25 mM, [TPMA] = 200 mM). The initiator OH-EBIB (4.2 mg, 0.02 mmol, 1 eq.) was added to the Schlenk flask by withdrawing an aliquot from a previously prepared stock solution in DMSO ([OH-EBIB] = 85 mg mL^{-1}). A stock solution of AA was prepared in a two-necks round bottom flask by firstly introducing dry AA (degassed with 3 vacuum/N_2 cycles), then adding degassed PBS 100 mM ([AA] = 5.28 mg mL^{-1}). An aliquot of AA stock solution (1.3526 mg, 0.00768 mmol, 0.384 eq.) was inserted in the Schlenk vial to start the polymerization. The reaction mixture was stirred at 30 °C for 18 h. The product was purified *via* dialysis against deionized water for 48 h (regenerated cellulose 3 kDa MWCO membranes, Spectra/Por®) and then freeze-dried. Yield > 90%. ^{1}H-NMR (400 MHz, D_2O), δ (ppm): 0.6–1.2 (m, 3H, CH_3COO), 1.96 (s, 2H, CH_2CCH_3), 3.65 (m, 2H, $CHCH_2OH$), 3.99 (m, H, OCH_2CH), 4–4.15 (m, 2H, $COOCH_2$).

2.4. Synthesis of P(PEGMA)$_n$ from commercial initiator

100 mL of PBS 100 mM were inserted in a two-necks round bottom flask, 3 cycles of vacuum/N_2 of 5 min each were performed followed by 15 min of N_2 purge. All reactants were used in the molar ratios reported below, expressed as equivalents with respect to the ATRP initiator. PEGMA monomer (2.5 g, 5 mmol, n eq., where $n = 250$) was inserted in a Schlenk vial and 3 vacuum/N_2 cycles of 5 min each were performed. 15.2 mL of degassed PBS 100 mM were added to the Schlenk vial, and the reaction mixture was left under continuous flow of N_2. The catalyst $CuBr_2$ (0.335 mg, 0.0015 mmol, 0.075 eq.) and the ligand TPMA (3.4843 mg, 0.012 mmol, 0.6 eq.) were added to the reaction mixture from a stock solution in PBS 100 mM ([$CuBr_2$] = 25 mM, [TPMA] = 200 mM). The initiator OH-EBIB (4.2 mg, 0.02 mmol, 1 eq.) was added to the Schlenk flask by withdrawing an aliquot from a previously prepared stock solution in DMSO ([OH-EBIB] = 85 mg mL^{-1}). A stock solution of AA was prepared in a two-necks round bottom flask by firstly introducing dry AA (degassed with 3 vacuum/N_2 cycles), then adding degassed PBS 100 mM ([AA] = 5.28 mg mL^{-1}). An aliquot of AA was withdrawn from the degassed stock solution (1.3526 mg, 0.00768 mmol, 0.384 eq.) to start the polymerization. The reaction mixture was stirred at 30 °C for 18 h. The product was purified *via* dialysis against deionized water for 48 h (regenerated cellulose 3 kDa MWCO membranes, Spectra/Por®) followed by freeze-drying. Yield > 90%. ^{1}H-NMR (400 MHz, D_2O), δ (ppm): 0.6–1.2 (m, 3H, CH_2CCH_3), 1.96 (s, 2H, CH_2CCH_3), 3.45 (m, 3H, CH_3CH_2), 3.6–3.9 (m, 54H, ($CH_2CH_2OCH_2$)), 3.9–4.4 (m, 2H, CH_2O).

2.5. Hydrolysis of PGMA$_m$

20 mg of PGMA$_m$ lyophilized polymer were placed in a round glass vial. Then, 2 mL of 3 M NaOH solution were added, and the vial was sealed with a crimped cap to maintain pressure during heating, preventing the solution from reaching its boiling point. The reaction mixture was stirred (400 rpm) in an oil bath heating system at 120 °C for 30 min, 1 h, 2 h, 4 h, 6 or 18 h to study the reaction progression over time. The resulting product was neutralized with HCl 3 M and dialyzed against deionized water for 48 h (regenerated cellulose 3.5 kDa MWCO membranes, Spectra/Por®). The content of the dialysis bag was filtered with filter paper and the recovered liquid was lyophilized. Yield 70%.

2.6. Hydrolysis of P(PEGMA)$_n$

60 mg of P(PEGMA)$_n$ lyophilized polymer were inserted in a rounded glass vial. Then, 2 mL of NaOH 3 M or NaOH 6 M solution were added, and the vial was sealed with a crimped cap to maintain pressure during heating, preventing the solution from reaching its boiling point. The reaction mixture was stirred (400 rpm) in an oil bath heating system at 120 °C for 30 min, 1 h, 2 h, 4 h, 6 or 18 h to study the reaction progression over time. The resulting product was neutralized with HCl 3 M and dialyzed against deionized water for 48 h (regenerated cellulose 3.5 kDa MWCO membranes, Spectra/Por®). The content of the dialysis bag was filtered with filter paper and the recovered liquid was lyophilized. Yield 70%.

2.7. Microwave-assisted hydrolysis of PGMA$_m$

20 mg of PGMA$_m$ or LYS-PGMA$_m$ lyophilized polymer were inserted in a microwave reaction glass vial (Biotage®), then 2 mL of NaOH 3 M solution were added prior to close the vial with a crimped cap. The solution was pre-stirred for 5 min and then warmed up inside a robot-equipped Biotage® Initiator + Microwave Synthesizer (Biotage®, Sweden AB) until reaching 120 °C (400 W). The reaction mixture was maintained under constant microwave irradiation and stirred for 5 min, 10 min, 15 min, 30 min, 1 h, 2 h or 3 h to study the reaction progression over time. At the end of the reaction, pressurized air was introduced inside the microwave cavity to rapidly cool the reaction mixture. The resulting product was neutralized with HCl 3 M and dialyzed against deionized water for (regenerated cellulose 3.5 kDa MWCO membranes, Spectra/Por®). The content of the dialysis bag was filtered with filter paper and the recovered liquid was lyophilized. Yield 70%.

2.8. Microwave-assisted hydrolysis of P(PEGMA)$_n$

60 mg of P(PEGMA)$_n$ or LYS-P(PEGMA)$_n$ lyophilized polymer were inserted in a microwave reaction glass vial (Biotage®), then 2 mL of NaOH 6 M solution were added prior to close the vial with a crimped cap. The solution was pre-stirred for 5 min and then warmed up inside a robot-equipped Biotage® Initiator + Microwave Synthesizer (Biotage®, Sweden AB) until reaching 120 °C (400 W). The reaction mixture was maintained under constant microwave irradiation and stirred for 30 min, 1 h, 2 h,

4 h, 6 h, 8 h, 14 h to study the reaction progression over time. At the end of the reaction, pressurized air was introduced inside the microwave cavity to rapidly cool the reaction mixture. The resulting product was neutralized with HCl 3 M and dialyzed against deionized water for 48 h (regenerated cellulose 3.5 kDa MWCO membranes, Spectra/Por®). The content of the dialysis bag was filtered with filter paper and the recovered liquid was lyophilized. Yield 70%.

3. Results and discussion

3.1. Polymer design and characterization

$PGMA_m$ and $P(PEGMA)_n$ polymers were synthesized *via* AGET ATRP conducted in aqueous solution (100 mM PBS), employing $CuBr_2$ or $CuCl_2$ as catalysts, TPMA as ligand, and ascorbic acid as the catalyst activator. The reactions were first performed with a commercial initiator (OH-EBiB) and later with functionalized hen egg white lysozyme (LYS-A1) as a model protein. The protein was chemically modified *via* reductive amination to functionalize its *N*-terminus with a bromine-containing group (Fig. 1) capable of serving as an ATRP initiator for the synthesis of the desired polymer. Detailed procedures for the modification and characterization are provided in previous publications.[34,35] The reaction scheme followed for the synthesis of the two polymers is shown in Fig. S1 (SI). Both $PGMA_m$ and $P(PEGMA)_n$ ATRP reached high conversions ($\chi \geq 90\%$ after 8 h), as confirmed by ^{1}H-NMR (Table 1).

For the synthesis of $PGMA_m$, a theoretical degree of polymerization (DP_{th}) of 125 units was initially chosen, while $P(PEGMA)_n$ was polymerized with a DP_{th} of 250 units. The resulting polymers were employed to study the hydrolysis kinetics using both microwave and conventional heating methods. $PGMA_m$ samples with variable lengths (DP_{th} = 80, 50, 20) were then produced in order to highlight how their different molecular weights were reflected in the SEC analysis of the corresponding hydrolyzed polymers. Polymerizations were subsequently adapted to employ LYS-A1 as the initiator where a target DP_{th} of 125 and 250 units was selected for the synthesis of $LYS-PGMA_m$. The synthetic procedure and reaction components remained unchanged from those optimized using the commercial initiator. The list of the studied macromolecules and their characterization data are summarized in Table 1.
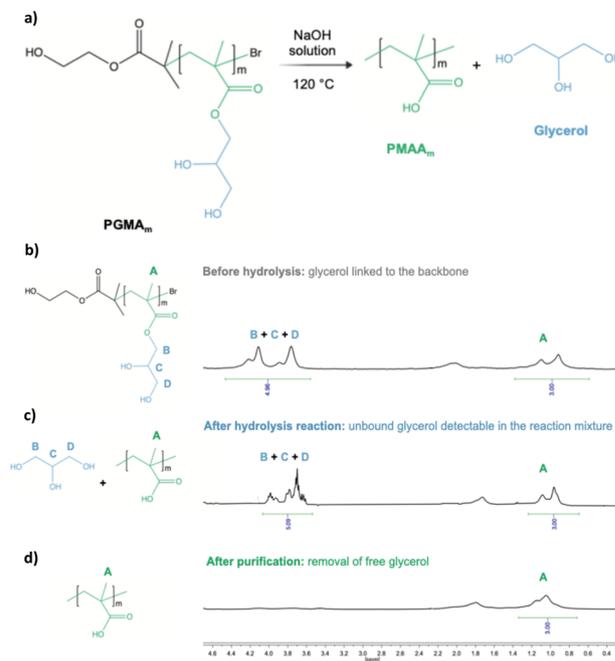

Fig. 2 (a) Base-catalyzed hydrolysis reaction of $PGMA_m$ esters bonds leading to the formation of $PMAA_m$ and glycerol. ^{1}H-NMR spectrum progression recorded: (b) before $PGMA_{112}$ hydrolysis, (c) after hydrolysis but prior to purification, and (d) after purification. The disappearance of signals corresponding to free glycerol in spectrum (d) confirms its successful detachment from the polymer backbone.

3.2. Hydrolysis of $PGMA_m$ homopolymer

Polymers with a methacrylic backbone typically undergo ester bond hydrolysis *via* a base-catalyzed reaction in aqueous solution at elevated temperatures. Basic conditions were preferred to ensure the solubility of PMAA formed during hydrolysis. This study investigated the kinetic profile of the hydrolysis of $PGMA_{112}$ (DP_{th} = 125, DP_{NMR} = 112, as reported in Table 1) conducted in a 3 M NaOH solution at 120 °C, utilizing both a microwave synthesizer and a conventional heating method, such as oil bath heating system with a thermocouple for temperature control.

To identify the minimum time required for complete hydrolysis, various reaction durations were tested for both

Table 1 Summary of properties of $PGMA_m$ and $P(PEGMA)_n$ polymers obtained from commercial initiator and LYS-A1. DP_{th} indicate the target degree of polymerization while DP_{NMR} represent the one actually achieved based on polymerization conversion calculated by ^{1}H-NMR (χ_{ATRP}). Number average molecular weight ($M_{n,NMR}$ and $M_{n,SEC}$) were obtained *via* ^{1}H-NMR and standard organic SEC analysis respectively, while the dispersity $Đ_{SEC}$ was evaluated *via* organic SEC. LYS-A1 M_n = 14.57 kDa

Polymer	DP_{th} [−]	DP_{NMR} [−]	χ_{ATRP} [%]	$M_{n,NMR}$ [kDa]	$M_{n,SEC}$ [kDa]	$Đ_{SEC}$ [−]
$PGMA_{112}$	125	112	90	18.1	22.1	1.3
$PGMA_{79}$	80	79	99	12.9	14.9	1.3
$PGMA_{46}$	50	46	92	7.6	9.3	1.2
$PGMA_{18}$	20	18	90	3.1	4.1	1.2
$P(PEGMA)_{245}$	250	245	98	122.7	147.3	1.3
$LYS-PGMA_{109}$	125	109	87	32.9	—	—
$LYS-PGMA_{175}$	250	175	70	42.6	—	—

methods. After each reaction, the resulting mixture was neutralized with HCl and dialyzed against deionized water, to remove salts formed during the neutralization and any residual glycerol, then analyzed by ^{1}H-NMR to determine the degree of conversion. As illustrated in Fig. 2a, the typicla hydrolysis mechanism of $PGMA_m$ led to the formation of linear poly(methacrylic acid) ($PMAA_m$) and glycerol. Accordingly, the output of the various reactions was quantified by calculating the ratio of the peak area (^{1}H-NMR spectrum recorded in D_2O) corresponding to glycerol bound to the backbone, measured prior to the hydrolysis reaction (denoted by labels 'B', 'C' and 'D' in Fig. 2b), and the area of the same peak after hydrolysis. This methodology enabled the determination of the percentage of glycerol detached from the main backbone as a result of the hydrolytic process.

By comparing the ^{1}H-NMR spectrum of the sample obtained after hydrolysis (prior to purification) (Fig. 2c) with that of the native $PGMA_m$ polymer, peaks associated with glycerol are still observed. In the spectrum recorded after purification (Fig. 2d), the free glycerol is absent, as evidenced by the lack of signals in the 3.4–4.2 ppm region, leaving only the peaks corresponding to the linear PMAA chain. Fig. 3a illustrates the kinetic profiles of the hydrolysis reactions conducted using both microwave irradiation and conventional oil bath heating. The data clearly demonstrate that the microwave-assisted process is significantly faster and more efficient, achieving complete hydrolysis of the treated polymer within just 1 hour. In contrast, the same

result was obtained only after 6 hours when using a standard oil bath. This outcome confirms that microwave irradiation has a pronounced effect in accelerating the process, even when the same basic conditions, concentrations, and temperature are used. The increased efficiency of microwave heating can be attributed to the uniform and rapid energy distribution provided, leading to faster molecular interactions and more efficient energy transfer to the system.

This results in a significantly shortened reaction time compared to conventional heating methods, where heat transfer is slower and less uniform.

To support these considerations, Fig. 3b and S2 (SI) present the sequences of ^{1}H-NMR spectra acquired prior to the hydrolysis of $PGMA_{112}$ and at various time intervals during the hydrolysis reactions, conducted using both microwave irradiation and oil bath heating, respectively. From the series of spectra, it is evident that the signals in the 3.4–4.4 ppm region (corresponding to the glycerol moieties bound to the polymer backbone – labels 'B', 'C', 'D') decrease significantly more rapidly over the course of the reaction when microwave irradiation is employed, compared to conventional conductive heating.

In parallel, Fig. 4 compares the FTIR spectra of the non-hydrolyzed $PGMA_{112}$ polymer and the products obtained from reactions of variable durations (15 min and 1 h) using the microwave-assisted heating system. Methylene and methyl stretching in the region between 2800 and 3000 cm^{-1} were observed in the non-hydrolyzed spectrum, corresponding to native PGMA aliphatic group frequencies. Characteristic peaks related to C–O–C esters at 1700 cm^{-1} were identified as well.

On the contrary, the spectrum of the hydrolyzed polymer shows significantly less prominent aliphatic chain signals (CH_2 and CH_3 around 2900 cm^{-1}) and a progressive disappearance of the ester-related peak (around 1700 cm^{-1}), in favor of the C=O
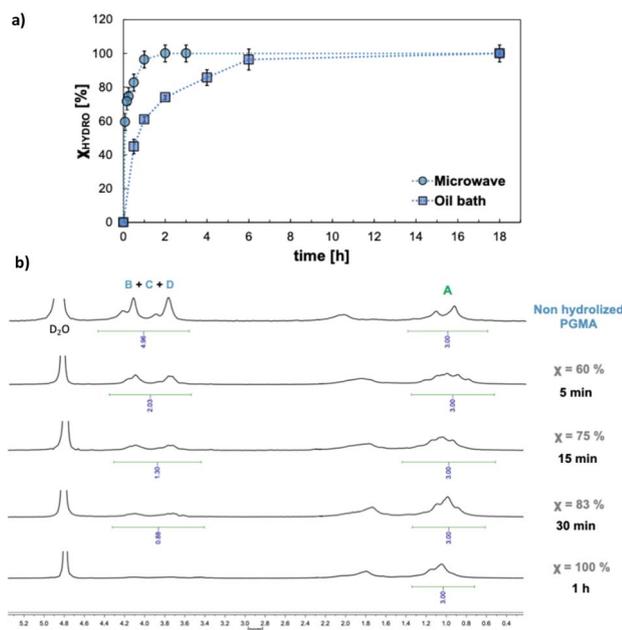

Fig. 3 (a) Kinetic profile of the hydrolysis reaction of $PGMA_{112}$ conducted under microwave irradiation and in an oil bath, expressed as conversion *versus* reaction time. Error bars represent the standard deviation calculated from three independent experiments. (b) Sequence of ^{1}H-NMR spectra recorded before the hydrolysis of $PGMA_{112}$ by means of a microwave reactor and after various reaction time points. Letters (A–D) refers to PGMA protons and corresponding ^{1}H-NMR peaks as reported in the structure shown in Fig. 2.
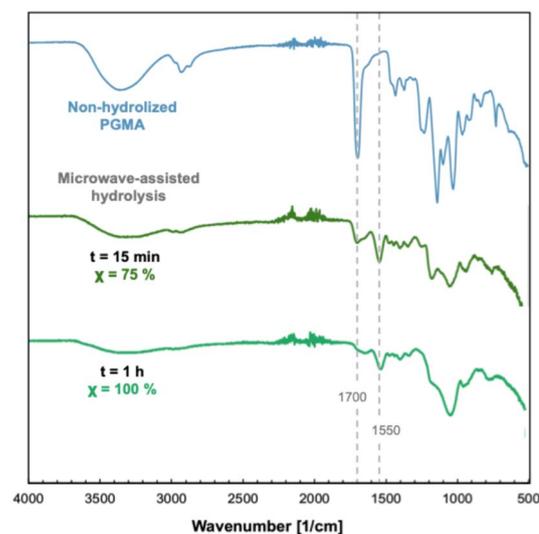

Fig. 4 FTIR spectrum progression recorded before $PGMA_{112}$ hydrolysis (light blue), after 15 min-hydrolysis leading to 75% of conversion (dark green) and after 1 h of hydrolysis (light green) achieving 100% of conversion employing a microwave synthesizer.

carbonyl stretching of carboxylates at around 1550 cm^{-1},[89,90] clearly indicates the increasing hydrolysis conversion with complete cleavage already achieved at 1 h. The FTIR spectra comparing the non-hydrolyzed PGMA$_{112}$ with the hydrolyzed polymer obtained *via* an oil-bath-based heating procedure are shown in Fig. S3 of the SI.

Both sets of analyses reported in Fig. 3 and in Fig. 4 demonstrate a clear time-dependent progression of the reaction. Notably, each reaction corresponding to different time points was performed in triplicate for both heating methods, ensuring the reliability and consistency of the findings.

3.3. Hydrolysis of LYS-PGMA$_m$ conjugate

In light of the successful hydrolysis results achieved for PGMA$_{112}$ employing both a microwave synthesizer and an oil bath-based heating system, previously optimized conditions were pursued to achieve the hydrolysis of LYS-PGMA$_m$ conjugate (DP$_{th}$ = 125, DP$_{NMR}$ = 109, as reported in Table 1). Firstly, the heating oil bath protocol was tested to verify its effectiveness, successively the reaction was translated to microwave-assisted protocol. The reaction product was analyzed through ^{1}H-NMR spectroscopy, which confirmed the same chemical shifts as those previously illustrated for hydrolyzed PGMA$_{112}$, attributed to the successful hydrolysis of the conjugate. Fig. 5 highlight the FTIR spectra of the non-hydrolyzed PGMA$_{112}$ polymer and the non-hydrolyzed LYS-PGMA$_{109}$ conjugate with the one of LYS-PGMA$_{109}$ after 1 h of hydrolysis in a microwave-assisted heating system. Methylene and methyl stretching in the region between 2800 and 3000 cm^{-1}, together with C–O–C esters peaks at 1700 cm^{-1} were observed in the non-hydrolyzed spectra of both PGMA$_{112}$ and LYS-PGMA$_{109}$. On the contrary, within the spectrum of the hydrolyzed polymer significantly less prominent

aliphatic chain (CH$_2$ and CH$_3$ around 2900 cm^{-1}) and the disappearance of the ester related peak (around 1700 cm^{-1}),[89,90] confirmed that LYS-PGMA$_{109}$ was successfully hydrolyzed in 1 h.

3.4. Hydrolysis of P(PEGMA)$_n$ homopolymer

In parallel with the experiments conducted using PGMA$_{112}$, hydrolysis tests were also performed on P(PEGMA)$_n$ polymer (DP$_{th}$ = 250, DP$_{NMR}$ = 245, as reported in Table 1). The general mechanism of hydrolysis of P(PEGMA)$_n$ leads to the formation of linear PMAA$_n$ and poly(ethylene glycol) methyl ether (PEG), resulting from the cleavage of the P(PEGMA) ester bonds, as depicted in Fig. 6a.

Preliminary experiments, involving hydrolysis of the polymer in an oil bath with a 3 M aqueous NaOH solution at 120 °C (same reaction condition employed for PGMA hydrolysis), yielded unsatisfactory results after 18 hours of reaction (conversion < 10%, data not shown). The enhanced stability of P(PEGMA) against hydrolysis may be due to the steric hindrance of PEG side chain, together with its tendency to dehydrate at temperatures higher than its lower critical solubility temperature (LCST) above 85–90 °C.[35,91,92] Consequently, subsequent investigations were conducted by increasing the molarity of the NaOH solution, raising the concentration to 6 M. Subsequent studies examined the kinetic profile of P(PEGMA)$_{245}$ hydrolysis
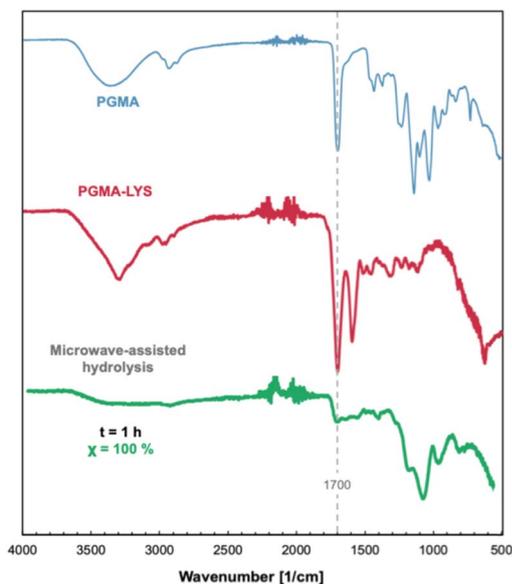

Fig. 5 Comparison of FTIR spectrum of PGMA$_{112}$ polymer from commercial initiator (light blue), LYS–PGMA$_{109}$ conjugate (red), and LYS-PGMA$_{109}$ after 1 h of hydrolysis leading to 100% of conversion (light green) employing a microwave synthesizer.
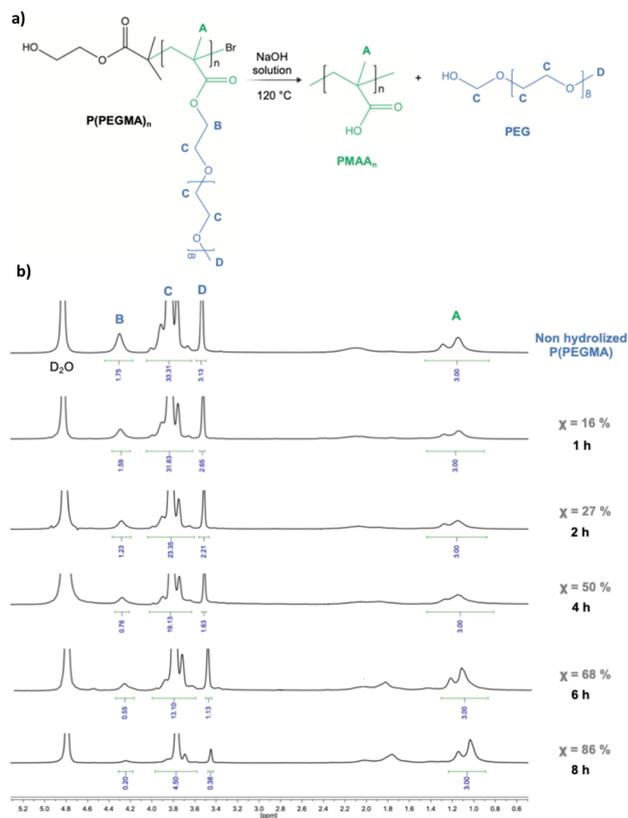

Fig. 6 (a) Base-catalyzed hydrolysis reaction of P(PEGMA)$_{245}$ esters bonds leading to the formation of PMAA$_{245}$ and PEG. (b) Sequence of ^{1}H-NMR spectra recorded before the hydrolysis of P(PEGMA)$_{245}$ by means of a microwave reactor and after various reaction time points.

in a 6 M NaOH solution at 120 °C, utilizing both a microwave synthesizer and a conventional oil bath, corresponding to the setups previously described.

Various reaction times were evaluated for both methods. Following each reaction, the resulting mixture was neutralized with HCl, dialyzed against deionized water to eliminate salts and the free PEG as by-product, and then analyzed by ^{1}H-NMR to assess the degree of conversion. The reaction outcome was quantified by calculating the ratio of the peak area (from the ^{1}H-NMR spectrum recorded in D_2O) corresponding to the PEG side chains attached to the backbone, measured before the hydrolysis reaction (denoted by labels 'B' and 'C' in Fig. 6), to the area of the same peak after hydrolysis. This approach allowed for the determination of the percentage of PEG detached from the main backbone as a result of the hydrolysis process. To confirm that the reaction led to the cleavage of the ester bond linking the PEG side chain to the PMAA backbone, the presence of the peak corresponding to the terminal methyl group of the PEG side chain ('D', δ = 3.5 ppm) was monitored. This ensured that cleavage did not occur in correspondence of the ether bonds of the ethylene glycol units. From the spectra depicted in Fig. 6b, it can be seen that, in the case of microwave irradiation, as the reaction time increased, the area of the peak corresponding to the methylene group of the PEG side chain attached to the backbone (3.2–4.4 ppm region) progressively decreased, reaching approximately 13% of its initial value. Meanwhile, the peak corresponding to the terminal methyl group of PEG remained proportionally coherent with respect to the other peaks (within the limits of integration error due to the processing of the ^{1}H-NMR spectra). Hence, it was evident that prolonged reaction times could increase the number of ester groups effectively cleaved. A similar trend was observed in the progression of spectra recorded for the reactions conducted in the oil bath (Fig. S4); however, in this case, the decrease in the area of peaks labeled as 'B', 'C' and 'D' is limited to a maximum of 20%.

Fig. 7 presents the kinetic profiles of P(PEGMA)$_{245}$ hydrolysis reactions conducted using both microwave irradiation and conventional oil bath heating. In both cases, it was not possible to achieve 100% hydrolysis; however, the best performance was clearly observed in the microwave-assisted process, which allowed approximately an average of 87% hydrolysis to be achieved within 8 hours. Despite attempts to increase the reaction time, after 14 hours the process reached a plateau, beyond
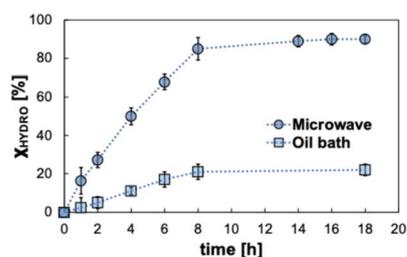
which no further improvements in performance were observed. In contrast, with standard heating, it was not possible to exceed 20% hydrolysis even after extending the reaction time to 18 hours. These results confirm that, at equal temperature and base concentration, microwave irradiation proves to be more effective than the oil bath method in favoring the hydrolysis process.

The incomplete hydrolysis of P(PEGMA), even under prolonged microwave irradiation, is consistent with previous observations and can be rationalized by a combination of structural and physicochemical factors that limit the hydrolysability of this polymer. The steric shielding provided by the PEG side chains is expected to progressively hinder hydroxide access to ester groups along the backbone as hydrolysis proceeds. In addition, at temperatures above the LCST of PEG-based polymers, partial dehydration and chain collapse may occur, promoting local densification or aggregation that further limits reagent diffusion. Such effects are likely exacerbated as the fraction of residual PEG side chains decreases, leading to a heterogeneous reaction environment and a plateau in conversion. Finally, variations in local microenvironment along the polymer chain may result in ester groups with different effective reactivities, making complete hydrolysis kinetically inaccessible under the investigated conditions.

In agreement with these findings, Fig. 8 compare the results obtained from FTIR spectroscopy of the non-hydrolyzed polymer and the products obtained from reactions of varying durations, from samples derived from both the microwave-assisted hydrolysis reaction (Fig. 8a) and the standard heating system (Fig. 8b). For the microwave-assisted reaction, carbonyl stretching peaks related to ester hydrolysis were observed around 1500 cm^{-1} for both the 4-hour and 8-hour samples. However, a significantly less intense ester-related signal around 1700 cm^{-1} was detected for the 8-hour reaction, indicating the breakdown of ester bonds over time. IR analysis thus confirmed the results obtained from NMR spectroscopy, validating the beneficial effects of prolonged reaction times. Concerning reactions conducted in oil bath, the spectrum of the non-hydrolyzed polymer exhibited CH_2 and CH_3 stretching vibrations around 2800–3000 cm^{-1}, which are characteristic of the methylene and methyl group frequencies of P(PEGMA). Furthermore, C–O–C stretching peaks, indicative of ester groups, were still observable around 1700 cm^{-1}. In line with the NMR data, the hydrolyzed product showed minimal changes compared to the native polymer.

3.5. Polymers characterization *via* SEC

As noted in Section 3.1, PGMA$_m$ samples with different molecular weights were synthesized (Table 1), including the one (PGMA$_{112}$) which was used to study hydrolysis kinetics under both microwave and conventional heating. These polymers were employed as calibration standards for determining the molecular weights of the hydrolyzed polymers under investigation. The native polymers were initially characterized using a SEC system working with DMAc as eluent. The analysis confirmed that the polymers exhibited the expected molecular

Fig. 7 Kinetic profile of the hydrolysis reaction of P(PEGMA)$_{245}$ conducted under microwave irradiation and in an oil bath, expressed as conversion *versus* reaction time. Error bars represent the standard deviation calculated from three independent experiments.
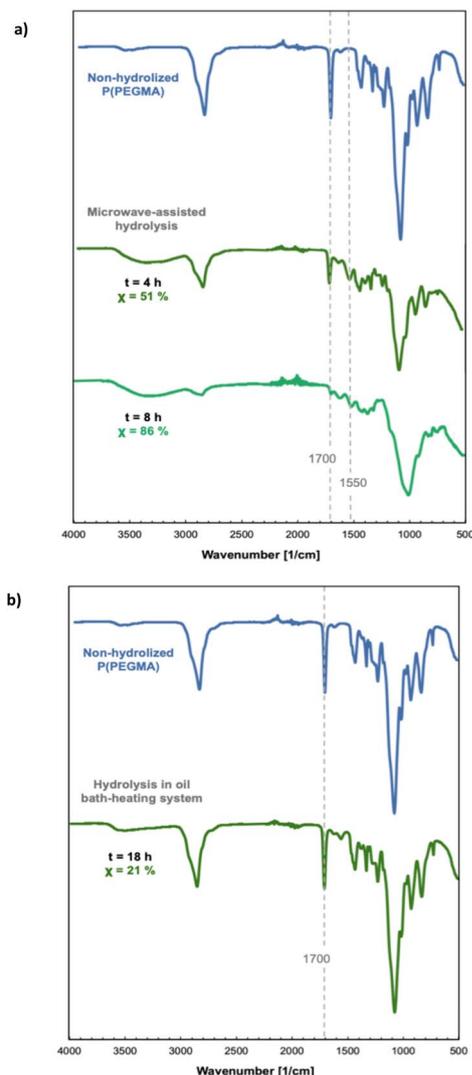
Fig. 8 FTIR spectrum progression recorded: (a) before P(PEGMA)$_{245}$ hydrolysis (light blue), after 4 h-hydrolysis in microwave leading to 51% of conversion (dark green) and after 8 h of hydrolysis (light green) achieving 87% of conversion; (b) before P(PEGMA)$_{245}$ hydrolysis (light blue) and after 18 h-hydrolysis using an oil bath-based heating system leading to 21% of conversion (dark green).

Fig. 9 (a) Normalized SEC chromatograms of four PGMA$_m$ samples with effective DP (DP$_{NMR}$) ranging from 18 to 112 GMA units. Analyses were performed in DMAc at a flow rate of 1.0 mL min^{-1}. (b) Normalized ASEC chromatograms of hydrolyzed PGMA$_m$ (m = 18, 46, 76, 112) resulting in PMAA$_m$. Analyses were performed in a phosphate-buffered NaNO$_3$ solution (pH 7) at a flow rate of 1.0 mL min^{-1}. (c) Correlation between the ASEC retention time of hydrolyzed PGMA$_m$ (m = 18, 46, 76, 112) (light blue), LYS-PGMA$_{109}$ (red) and P(PEGMA)$_{245}$ (blue) samples and the logarithm of the PMAA expected molecular weight (circles) and degree of polymerization (squares) after hydrolysis based on ^{1}H-NMR analysis of the synthesized polymers.

weights and narrow dispersity ($Đ_{SEC} < 1.3$), consistent with the controlled polymerization characteristics of ATRP. Their characterization data are reported in Table 1. Minor discrepancies between molecular weights determined by SEC and those calculated from ^{1}H-NMR are attributed to inherent limitations of the SEC system and the use of polystyrene calibration standards. Nevertheless, the deviation did not exceed a factor of 1.2. The chromatograms obtained from SEC analysis in DMAc for the four PGMA samples used as standards are shown in Fig. 9a. As expected, an increase in molecular weight corresponds to a decrease in retention time, clearly illustrating the inverse relationship between these two variables in the employed chromatographic system. This series of PGMA$_m$ samples was hydrolyzed using the optimized MAH protocol described in Section 3.2, employing microwave heating for 1 hour (the
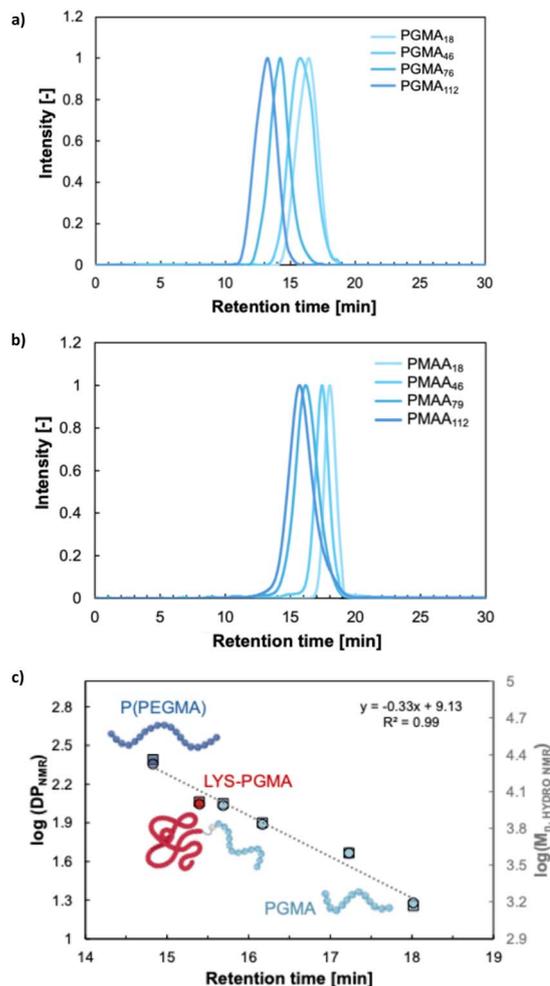
minimum time required to achieve complete hydrolysis). The resulting polymers were analyzed by aqueous SEC (ASEC) employing a phosphate-buffered NaNO$_3$ solution (pH 7) as the mobile phase. From the ASEC chromatograms (Fig. 9b), the retention times corresponding to each sample were derived. Fig. 9c correlates the logarithm of the expected molecular weight (as well as of the DP) of the hydrolyzed PGMA$_m$ polymers (based on ^{1}H-NMR analysis of the corresponding unhydrolyzed samples) with their actual retention times recorded by ASEC. As expected, a linear relationship was observed, consistent with a typical SEC calibration curve. Similarly, the hydrolyzed LYS-PGMA$_{109}$ conjugates (obtained via 1 h MAH in 3 M NaOH) and the P(PEGMA)$_{245}$ polymer hydrolyzed to approximately 90% (after 14 hours under microwave heating in 6 M NaOH solution)

Table 2 Molar mass characterization of linear polymers and lysozyme-conjugated polymers, obtained by MAH followed by ASEC. DP_{NMR} and $M_{n,NMR}$ (degree of polymerization and number average molecular weight) were calculated from ATRP monomer conversion determined by ^{1}H-NMR. DP_{HYDRO} and $M_{n,ASEC}$ were obtained by ASEC. The dispersity $Đ_{ASEC}$ was obtained by ASEC and it is referred to the hydrolysed polymers

Polymer	DP_{NMR} [−]	DP_{HYDRO} [−]	$M_{n,NMR}$ [kDa]	$M_{n,ASEC}$ [kDa]	$Đ_{ASEC}$ [−]
$PGMA_{112}$	112	108	18.1	17.5	1.3
$P(PEGMA)_{245}$	245	196	122.7	98.2	1.3
$LYS-PGMA_{109}$	109	109	17.6	17.4	1.3
$LYS-PGMA_{175}$	175	169	28.2	27.0	1.4

were also analyzed by ASEC. The retention times obtained for these samples exhibited the same linear correlation with the $\log(DP_{NMR})$ and $\log(M_{n,HYDRO\ NMR})$, as previously observed for the $PGMA_m$ sample series. Notably, in Fig. 9c the red and blue points, corresponding to the $LYS-PGMA_{109}$ and $P(PEGMA)_{245}$ samples respectively, fall precisely on the same trendline defined by the $PGMA_m$ series. These results demonstrate that hydrolyzed polymers with a predetermined degree of polymerization can serve as effective calibrants for determining the molar mass of both free and conjugated polymer samples after hydrolysis.

This approach is supported by the fact that, regardless of the initiator or monomer used, the hydrolysis of this polymer family consistently yields PMAA, which is isolated in its solid sodium salt form prior to dissolution and analysis by SEC. Since the degree of ionization of PMAA, which directly influences its hydrodynamic volume, can vary depending on factors such as the initial number of sodium carboxylate groups, pH, and ionic strength, the use of standard hydrophilic calibration polymers (such as PEG) may not be appropriate. These standards often differ significantly in hydrodynamic behaviour from the hydrolyzed polymers, potentially leading to inaccuracies in molar mass determination.

Once the MAH method and ASEC analysis were established, molar mass characterization was performed for $PGMA_{112}$ and $P(PEGMA)_{245}$ (previously employed for establishing hydrolisis kinetics, Section 3.2 and 3.4, respectively), and two lysozyme-$PGMA_m$ conjugates: $LYS-PGMA_{109}$, already used for prooving hydrolisis feasibilty on biological conjugates (Section 3.3), and an additional congiuate $LYS-PGMA_{175}$ (Table 2). The average degree of polymerization and number-average molecular weight determined by this MAH-ASEC method were consistent with values estimated via ^{1}H-NMR (based on ATRP monomer conversion). The differences were within 5% for $PGMA_m$ and around 20% for $P(PEGMA)_n$, the latter slightly higher, likely due to incomplete hydrolysis of PEG side chains, estimated at around 90%.

4. Conclusions

This work demonstrated the successful development of a robust and efficient methodology for determining the molar mass of functional polymers synthesized via controlled/living polymerization. By applying MAH to selectively cleave ester side chains, the polymers were converted into linear PMAA, enabling accurate molar mass characterization via ASEC. The study systematically optimized the hydrolysis conditions, showing that microwave heating significantly enhances reaction efficiency and conversion compared to conventional methods. This approach proved effective across a range of samples, including homopolymers such as PGMA and P(PEGMA), as well as their protein–polymer conjugates synthesized using ATRP, confirming its broad applicability. A comprehensive evaluation of hydrolysis kinetics under both conventional and microwave-assisted conditions confirmed that microwave heating greatly accelerates the process without compromising the integrity of the polymer backbone. Notably, P(PEGMA) hydrolysis was significantly more challenging than that of PGMA due to the stabilizing effect of its PEG side chains. While conventional heating yielded limited conversion even over extended times, microwave-assisted heating dramatically enhanced efficiency, making an otherwise impractical process feasible. The resulting polymers were thoroughly characterized using ^{1}H-NMR, FTIR, and SEC, establishing reliable correlations between molecular weight and retention time. Overall, the MAH-ASEC method provides a powerful, scalable strategy for precise molar mass determination, particularly in complex or protein-conjugated architectures, with high reproducibility and analytical clarity. Moreover, this approach offers a versatile platform for tuning polymer properties in biomedical and materials science applications.

Author contributions

Ilaria Porello: conceptualization, data curation, investigation, methodology, writing – original draft, writing – review & editing. Filippo Moncalvo: conceptualization, investigation, methodology. Paola Nastri: investigation, methodology. Marta Bozzi: investigation. Philippe Gonzalez: investigation. Alessandro Sacchetti: investigation, methodology. Francesco Cellesi: funding acquisition, supervision, conceptualization, data curation, investigation, methodology, writing – original draft, writing – review & editing.

Conflicts of interest

There are no conflicts to declare.

Data availability

The data supporting the findings of this study are available within the article and its supplementary information (SI).

Acknowledgements

References

1 Y. Gao, J. Remón and A. S. Matharu, *Green Chem.*, 2021, **23**, 3502–3525.

2 J. R. Lill, E. S. Ingle, P. S. Liu, V. Pham and W. N. Sandoval, *Mass Spectrom. Rev.*, 2007, **26**, 657–671.

3 K. Belkhir, G. Riquet and F. Becquart, *J. Chem.*, 2022, **2022**, 3961233.

4 M. Nüchter, B. Ondruschka, W. Bonrath and A. Gum, *Green Chem.*, 2004, **6**, 128–141.

5 A. de la Hoz, À. Díaz-Ortiz and A. Moreno, *Chem. Soc. Rev.*, 2005, **34**, 164–178.

6 D. Dallinger and C. O. Kappe, *Chem. Rev.*, 2007, **107**(6), 2563–2591.

7 J. Jacob, *Int. J. Chem.*, 2012, **4**, 29–41.

8 N. Sweygers, N. Alewaters, R. Dewil and L. Appels, *Sci. Rep.*, 2018, **8**, 7716.

9 Q. Liu, W. Q. He, M. Aguedo, X. Xia, W. B. Bai, Y. Y. Dong, J. Q. Song, A. Richel and D. Goffin, *Carbohydr. Polym.*, 2020, **250**, 117170.

10 N. Wang, A. Xu, K. Liu, Z. Zhao, H. Li and X. Gao, *Chem. Eng. J.*, 2024, **481**, 148786.

11 A. T. Hoang, S. Nižetić, H. C. Ong, M. Mofijur, S. F. Ahmed, B. Ashok, V. T. V. Bui and M. Q. Chau, *Chemosphere*, 2021, **286**, 130878.

12 S. K. Ulug, F. Jahandideh and J. Wu, *Trends Food Sci. Technol.*, 2021, **108**, 27–39.

13 A. Görgüç, E. Gençdağ and F. M. Yılmaz, *Food Res. Int.*, 2020, **137**, 109504.

14 L. Kunlan, X. Lixin, L. Jun, C. Guoying and X. Zuwei, *Starch/Staerke*, 2001, **331**, 9–12.

15 A. Ajavakom, S. Supsvetson, A. Somboot and M. Sukwattanasinitt, *Carbohydr. Polym.*, 2012, **90**, 73–77.

16 E. Rieger, T. Gleede, A. Manhart, M. Lamla and F. R. Wurm, *ACS Macro Lett.*, 2018, **7**, 598–603.

17 S. Dutta, S. De, M. I. Alam, M. M. Abu-Omar and B. Saha, *J. Catal.*, 2012, **288**, 8–15.

18 Z. M. A. Bundhoo, *Renew. Sustain. Energy Rev.*, 2018, **82**, 2029–2038.

19 J. J. Rubio Arias and W. Thielemans, *Green Chem.*, 2021, **23**, 9945–9956.

20 B. Guo, X. Lopez-Lorenzo, Y. Fang, E. Bäckström, A. J. Capezza, S. R. Vanga, I. Furó, M. Hakkarainen and P. O. Syrén, *ChemSusChem*, 2023, **16**(18), e202301237.

21 Z. Bouhsain, S. Garrigues, A. Morales-Rubio and M. de la Guardia, *Anal. Chim. Acta*, 1996, **330**, 59–69.

22 C. Xu and B. Li, *Spectrochim. Acta, Part A*, 2004, **60**, 1861–1864.

23 M. Larhed and A. Hallberg, *Chem. Rev.*, 2001, **101**, 406–416.

24 V. J. Parekh, V. K. Rathod and A. B. Pandit, *Compr. Biotechnol.*, 2011, **2**, 104–118.

25 H. G. Barth, B. E. Boyes and C. Jackson, *J. Chromatogr., A*, 1996, **68**, 445–466.

26 I. Porello and F. Cellesi, *Front. Bioeng. Biotechnol.*, 2023, **11**, 1211798.

27 I. Porello, N. Bono, G. Candiani and F. Cellesi, *Polym. Chem.*, 2024, **15**, 2800–2826.

28 L. A. Canalle, D. W. P. M. Löwik and J. C. M. van Hest, *Chem. Soc. Rev.*, 2010, **39**, 329–353.

29 R. M. Broyer, G. N. Grover and H. D. Maynard, *Chem. Commun.*, 2011, **47**, 2212–2226.

30 J. Gonzalez-Valdivieso, A. Girotti, J. Schneider and F. J. Arias, *Int. J. Pharm.*, 2021, **600**, 120438.

31 C. Chen, D. Y. W. Ng and T. Weil, *Prog. Polym. Sci.*, 2020, **105**, 101241.

32 K. M. Burridge, B. A. Shurina, C. T. Kozuszek, R. F. Parnell, J. S. Montgomery, J. L. Vanpelt, N. M. Daman, R. M. McCarrick, T. A. Ramelot, D. Konkolewicz and R. C. Page, *Chem. Sci.*, 2020, **11**, 6160–6166.

33 S. Jevševar, M. Kunstelj and V. G. Porekar, *Biotechnol. J.*, 2010, **5**, 113–128.

34 F. Moncalvo, E. Lacroce, G. Franzoni, A. Altomare, E. Fasoli, G. Aldini, A. Sacchetti and F. Cellesi, *React. Funct. Polym.*, 2022, **178**, 105264.

35 F. Moncalvo, E. Lacroce, G. Franzoni, A. Altomare, E. Fasoli, G. Aldini, A. Sacchetti and F. Cellesi, *Macromolecules*, 2022, **55**(17), 7454–7468.

36 I. Lacík, S. Beuermann and M. Buback, *Macromolecules*, 2003, **36**, 9355–9363.

37 F. D. Kuchta, A. M. van Herk and A. L. German, *Macromolecules*, 2000, **33**, 3641–3649.

38 S. Beuermann, M. Buback, P. Hesse, R. A. Hutchinson, S. Kukučková and I. Lacík, *Macromolecules*, 2008, **41**, 3513–3520.

39 M. Buback, P. Hesse, R. A. Hutchinson, P. Kasák, I. Lacík, M. Stach and I. Utz, *Ind. Eng. Chem. Res.*, 2008, **47**, 8197–8204.

40 R. J. Minari, G. Cáceres, P. Mandelli, M. M. Yossen, M. González-Sierra, J. R. Vega and L. M. Gugliotta, *Macromol. React. Eng.*, 2011, **5**, 223–231.

41 R. P. Lattimer, *J. Anal. Appl. Pyrolysis*, 2003, **68–69**, 3–14.

42 P. Knappe, R. Bienert, S. Weidner and A. F. Thünemann, *Macromol. Chem. Phys.*, 2010, **211**, 2148–2153.

43 N. F. G. Wittenberg, M. Buback, M. Stach and I. Lacík, *Macromol. Chem. Phys.*, 2012, **213**, 2653–2658.

44 Q. Y. Li, Z. F. Yao, J. Y. Wang and J. Pei, *Rep. Prog. Phys.*, 2021, **84**, 076601.

45 E. A. Grulke, E. H. Immergut and J. Brandrup, *Polym. Handbook*, 2004.

46 F. Rodríguez-Ropero, T. Hajari and N. F. A. van der Vegt, *J. Phys. Chem. B*, 2015, **119**, 15780–15788.

47 M. Kovaliov, M. L. Allegrezza, B. Richter, D. Konkolewicz and S. Averick, *Polymer*, 2018, **137**, 338–345.

48 E. M. Pelegri-O'Day and H. D. Maynard, *Acc. Chem. Res.*, 2016, **49**, 1777–1785.

49 S. A. Mohammad, S. Dolui, D. Kumar, S. R. Mane and S. Banerjee, *Polym. Chem.*, 2021, **12**, 3042–3051.

50 S. Lee, J. Park, H. Ma, W. Kim, Y. K. Song, D. W. Lee, S. M. Noh, S. J. Yoon and C. Yang, *ACS Appl. Mater. Interfaces*, 2024, **16**, 5138–5148.

51 I. Porello, F. Stucchi, R. Guarini, G. Sbaruffati and F. Cellesi, *Biomacromolecules*, 2025, **26**(8), 5269–5286.

52 A. Blanazs, A. J. Ryan and S. P. Armes, *Macromolecules*, 2012, **45**, 5099–5107.

53 S. J. Hunter, J. R. Lovett, O. O. Mykhaylyk, E. R. Jones and S. P. Armes, *Polym. Chem.*, 2021, **12**, 3629–3639.

54 C. P. Jesson, V. J. Cunningham, M. J. Smallridge and S. P. Armes, *Macromolecules*, 2018, **51**, 3221–3232.

55 M. Kato, M. Kamigaito, M. Sawamoto and T. Higashimura, *Macromolecules*, 1995, **28**, 1721–1723.

56 I. Porello, F. Stucchi, G. Sbaruffati and F. Cellesi, *Eur. Polym. J.*, 2024, **220**, 113455.

57 O. Dechy-Cabaret, B. Martin-Vaca and D. Bourissou, *Chem. Rev.*, 2004, **104**, 6147–6176.

58 C. J. Hawker, A. W. Bosman and E. Harth, *Chem. Rev.*, 2001, **101**, 3661–3688.

59 J. Nicolas, Y. Guillaneuf, C. Lefay, D. Bertin, D. Gigmes and B. Charleux, *Prog. Polym. Sci.*, 2013, **38**, 63–235.

60 D. Cohen-Karni, M. Kovaliov, T. Ramelot, D. Konkolewicz, S. Graner and S. Averick, *Polym. Chem.*, 2017, **8**, 3992–3998.

61 L. Ragupathy, D. G. Millar, N. Tirelli and F. Cellesi, *Macromol. Biosci.*, 2014, **14**, 1528–1538.

62 M. Save, J. V. M. Weaver, S. P. Armes and P. McKenna, *Macromolecules*, 2002, **35**, 1152–1159.

63 S. Averick, A. Simakova, S. Park, D. Konkolewicz, A. J. D. Magenau, R. A. Mehl and K. Matyjaszewski, *ACS Macro Lett.*, 2012, **1**, 6–10.

64 B. S. Sumerlin, *ACS Macro Lett.*, 2012, **1**, 179–182.

65 M. S. Messina, K. M. M. Messina, A. Bhattacharya, H. R. Montgomery and H. D. Maynard, *Prog. Polym. Sci.*, 2020, **100**, 101176.

66 M. Tully, M. Dimde, C. Weise, P. Pouyan, K. Licha, M. Schirner and R. Haag, *Biomacromolecules*, 2021, **22**, 1406–1416.

67 G. Robert-Nicoud, R. Evans, C. D. Vo, C. J. Cadman and N. Tirelli, *Polym. Chem.*, 2013, **4**, 3458–3470.

68 E. Patrucco, S. Ouasti, D. V. Cong, P. De Leonardis, A. Pollicino, S. P. Armes, M. Scandola and N. Tirelli, *Biomacromolecules*, 2009, **10**, 3130–3140.

69 K. Mequanint, A. Patel and D. Bezuidenhout, *Biomacromolecules*, 2006, **7**, 883–891.

70 P. De Leonardis, F. Cellesi and N. Tirelli, *Colloids Surf., A*, 2019, **573**, 123734.

71 F. Moncalvo, M. I. Martinez Espinoza and F. Cellesi, *Front. Bioeng. Biotechnol.*, 2020, **8**, 89.

72 S. Rimmer, C. Johnson, C. Zhao, N. J. Zhao and S. Macneil, *Biomaterials*, 2007, **28**(34), 5050–5062.

73 R. Haigh, S. Rimmer and N. J. Fullwood, *Biomaterials*, 2007, **28**(36), 5392–5402.

74 C. Giacomelli, V. Schmidt and R. Borsali, *Macromolecules*, 2007, **40**, 2148–2157.

75 J. Morgenstern, G. Gil Alvaradejo, N. Bluthardt, A. Beloqui, G. Delaittre and J. Hubbuch, *Biomacromolecules*, 2018, **19**, 4250–4262.

76 Y. Kaneda, Y. Tsutsumi, Y. Yoshioka, H. Kamada, Y. Yamamoto, H. Kodaira, S. I. Tsunoda, T. Okamoto, Y. Mukai, H. Shibata, S. Nakagawa and T. Mayumi, *Biomaterials*, 2004, **25**, 3259–3266.

77 C. Pelosi, C. Duce, F. R. Wurm and R. T. Maria, *Biomacromolecules*, 2021, **22**, 1932–1943.

78 T. Steinbach, G. Becker, A. Spiegel, T. Figueiredo, D. Russo and F. R. Wurm, *Macromol. Biosci.*, 2017, **17**, 1600377.

79 J. Kopeček and P. Kopečková, *Adv. Drug Deliv. Rev.*, 2010, **62**, 122–149.

80 Y. Li and S. P. Armes, *Angew. Chem., Int. Ed.*, 2010, **49**, 4042–4046.

81 M. Ouchi, H. Yoda, T. Terashima and M. Sawamoto, *Polym. J.*, 2012, **44**, 51–58.

82 H. Jiang, C. Tian, L. Zhang, Z. Cheng and X. Zhu, *RSC Adv.*, 2014, **4**, 52430–52437.

83 A. Simakova, S. E. Averick, D. Konkolewicz and K. Matyjaszewski, *Macromolecules*, 2012, **45**, 6371–6379.

84 W. Jakubowski and K. Matyjaszewski, *Angew. Chem., Int. Ed.*, 2006, **45**, 4482–4486.

85 W. Jakubowski, K. Min and K. Matyjaszewski, *Macromolecules*, 2006, **39**, 39–45.

86 H. Dong, W. Tang and K. Matyjaszewski, *Macromolecules*, 2007, **40**, 2974–2977.

87 S. S. Cutié, P. B. Smith, D. E. Henton, T. L. Staples and C. Powell, *J. Polym. Sci. B*, 1997, **35**, 2029–2047.

88 G. Bokias, A. Durand and D. Hourdet, *Macromol. Chem. Phys.*, 1998, **199**, 1387–1392.

89 K. L. Thompson, S. P. Armes, D. W. York and J. A. Burdis, *Macromolecules*, 2010, **43**, 2169–2177.

90 J. Coates, *Encyclopedia of Analytical Chemistry*, 2000.

91 J. F. Lutz, *J. Polym. Sci., Part A*, 2008, **46**, 3459–3470.

92 J. F. Lutz, *Adv. Mater.*, 2011, **23**, 2237–2243.